

Evidence for radio-source heating of groups

J. H. Croston^{1,2?}, M.J. Hardcastle^{1,3} and M. Birkinshaw¹

¹ *H. H. Wills Physics Laboratory, University of Bristol, Tyndall Avenue, Bristol BS8 1TL*

² *Service d'Astrophysique, CEA Saclay, L'Orme des Merisiers, Bât. 709, 91191 Gif-sur-Yvette, France*

³ *School of Physics, Astronomy and Mathematics, University of Hertfordshire, College Lane, Hatfield, Hertfordshire AL10 9AB*

11 April 2024

ABSTRACT

We report evidence that the gas properties of X-ray groups containing radio galaxies differ from those of radio-quiet groups. For a well-studied sample of *ROSAT*-observed groups, we found that more than half of the elliptical-dominated groups can be considered “radio-loud”, and that radio-loud groups are likely to be hotter at a given X-ray luminosity than radio-quiet groups. We tested three different models for the origin of the effect and conclude that radio-source heating is the most likely explanation. We found several examples of groups where there is strong evidence from *Chandra* or *XMM-Newton* images for interactions between the radio source and the group gas. A variety of radio-source heating processes are important, including shock-heating by young sources and gentler heating by larger sources. The heating effects can be longer-lasting than the radio emission. We show that the sample of X-ray groups used in our study is not significantly biased in the fraction of radio-loud groups that it contains. This allows us to conclude that the energy per particle that low-power radio galaxies can inject over the group lifetime is comparable to the requirements of structure formation models.

Key words: galaxies: active – X-rays: galaxies: clusters

1 INTRODUCTION

Radio galaxies must be transferring large quantities of energy to the surrounding group- or cluster-scale gas. The P dV work done on the gas by source expansion is of the order of $10^{52} - 10^{53}$ J for source ages $\sim 10^8$ years (e.g. Croston et al. 2003). The first strong evidence for radio-source heating was recently found in the nearest radio galaxy, Centaurus A (Kraft et al. 2003): *Chandra* observations reveal a prominent shell of emission capping the inner southwestern radio lobe, which has a temperature ten times that of the surrounding galactic atmosphere, providing strong evidence that Cen A is shock-heating its atmosphere. There is also evidence for heating in the powerful FR II radio galaxy, Cygnus A (Smith et al. 2002), where a slight temperature increase in the X-ray gas is seen at the front edges of the lobe cavities. Another recent result helps to emphasise that more than one energy transfer mechanism is likely to operate. Deep *Chandra* observations (Fabian et al. 2003) of the Perseus cluster [the first cluster where “cavities” were observed (Böhringer et al. 1993)] have revealed the presence of ripples in the cluster gas that are suggestive of sound waves emanating from the central radio source, 3C 84. Fabian et al. calculate that the time scale between successive wavefronts is comparable to estimates of the radio-source lifetime, so that it seems plausible that an intermittent radio source is producing the observed ripples.

There is evidence that energy injection of some sort is required

to explain the observational properties of X-ray groups and clusters, which do not agree with the predictions of CDM models of structure formation (e.g. Arnaud and Evrard 1999; Ponman et al. 1999). Several authors have considered the effects of heating due to feedback from star formation (e.g. Balogh et al. 1999; Brighenti and Mathews 2001). However, in most cases it is found that heating from star formation and supernovae does not provide sufficient energy to explain the properties of both groups and clusters (e.g. Kravtsov and Yepes 2000). Wu et al. (2000) find that supernova heating can generate only $\sim 1/10$ of the energy required. These results have led many authors to consider AGN heating. Churazov et al. (2001) and Böhringer et al. (2002) consider the effects of radio-galaxy heating on cluster structure and conclude that sufficient heating could be provided. Evidence from recent observations of clusters, as well as simulations, suggest that AGN could provide a sufficiently distributed heating mechanism for this method to work (e.g. Brüggen and Kaiser 2002; Fabian et al. 2003), which removes a long-standing objection to radio-source heating models. Since radiative cooling in the absence of feedback overpredicts the mass in galaxies (e.g. Cole 1991), it seems likely that some sort of feedback is required to explain observed cluster properties and the galaxy luminosity function (e.g. Voit and Bryan 2001; Benson et al. 2003; Kay 2004).

In addition, nearly all cooling-flow clusters contain a central radio galaxy (e.g. Eilek 2004), and there is considerable evidence that the radio galaxy displaces gas in the cooling-flow regions (e.g. Böhringer et al. 1993; Blanton et al. 2001; Fabian et al. 2003). It

? Email: jcroston@discovery.saclay.cea.fr

is therefore important to consider the different means by which radio galaxies could influence the observed properties of the cooling flow, and in particular whether they can help explain why large quantities of gas do not appear to cool past $\sim 1=3$ the outer cluster temperature (e.g. Peterson et al. 2003; Sakelliou et al. 2002). Although non-heating solutions to this problem exist, it is most plausible that the bulk of the gas in these systems is reheated by one of several possible mechanisms, such as cluster mergers, thermal conduction (e.g. Voigt et al. 2002; Voigt and Fabian 2004), or AGN heating (Binney and Tabor 1995; Brüggen and Kaiser 2001, 2002; Reynolds et al. 2002); the last of these is particularly attractive because of the possibility of self-regulation via feedback. Investigating how radio galaxies can affect their hot-gas environments is therefore important to our understanding of several problems of cluster physics.

In Croston et al. (2003), we showed that radio galaxies have an important impact on groups, and found evidence that the properties of “radio-loud” and “radio-quiet” groups differ, in the sense that “radio-loud” groups are hotter than “radio-quiet” groups of comparable X-ray luminosity. That work used a fairly small and inhomogeneous sample, and the analysis methods were comparatively basic. Here we present a detailed analysis of a larger, homogeneous sample of groups (Osmond and Ponman 2004) in order to confirm and investigate further the conclusions of the earlier work.

2 SAMPLE SELECTION AND ANALYSIS

2.1 The elliptical-dominated sample

This analysis uses the GEMS group sample whose X-ray properties were presented by Osmond and Ponman (2004) (hereafter OP04). The sample consists of 60 groups, including loose and compact groups that may be spiral- or elliptical-dominated. For the larger GEMS sample, the $L_X = T_X$ relation shows more scatter than for the earlier work of Helsdon and Ponman (2000), so that it may be more difficult to distinguish heating effects.

We considered only the subset of groups in the OP04 sample that contain a large elliptical galaxy, as spiral-dominated groups are unlikely to possess a strong radio galaxy. We found that the scatter in the $L_X = T_X$ relation is significantly reduced in our subsample, suggesting that spiral-dominated groups have different gas properties from those with a large elliptical galaxy. OP04 did not report a significant difference in the $L_X = T_X$ properties of elliptical- and spiral-dominated groups; however, they do find that most X-ray bright groups contain a bright central early-type galaxy. They used the group’s spiral fraction to compare group properties. Our classification on the basis of the dominant galaxy’s morphology may be a more useful measure of the group’s history and current properties. This is supported by OP04’s conclusions about the importance of elliptical brightest group galaxies.

In order to determine whether each group contains a large elliptical galaxy, we downloaded DSS2 (Digitized Sky Survey¹) images of each group. Typically groups were either dominated by one large galaxy, or else there were several bright galaxies of similar magnitude. In the first case, we rejected any groups whose dominant galaxy is a spiral or S0. In the second case, where there was no obviously dominant galaxy, the group was only rejected if *none* of the bright galaxies is an elliptical. In some cases it

was not possible to tell by eye whether a galaxy has an elliptical or S0 morphology, and so we followed up all of the elliptical groups using Simbad and NED to confirm the galaxy morphology. Unfortunately there are many cases where these databases disagree, and multiple classifications exist in the literature. We therefore only rejected groups where the ambiguous galaxy was classified as S0 by both Simbad and NED. In all we excluded 15 spiral-dominated groups: HCG 10, HCG 15, HCG 16, HCG 40, HCG 68, HCG 92, NGC 1332, NGC 2563, NGC 3227, NGC 3396, NGC 4565, NGC 4725, NGC 5689, NGC 5907 and NGC 6574. In the course of following up galaxy morphologies, we also found one group, HCG 22, for which the supposed group members covered an implausibly large range in redshift. As it is unclear which galaxies are real members of this group, we excluded it as well.

In addition to excluding spiral-dominated groups, we also had to exclude 10 groups for which OP04 could not make X-ray spectral measurements: HCG 4, HCG 48, HCG 58, NGC 1808, NGC 3640, NGC 3783, NGC 4151, NGC 4193, NGC 6338 and NGC 7714. As the aim of the study was to compare the properties of radio-loud and radio-quiet groups, we also had to exclude two groups with low declinations that are not covered by the surveys used to identify the radio sources, NGC 1566 and NGC 7144. Finally, NGC 315 was excluded, because Worrall et al. (2003) find a dominant contribution to the X-ray luminosity from the AGN and X-ray jet, and HCG 67 was excluded because of ambiguity in whether or not an identified nearby radio source is actually associated with the group. The final sample of elliptical-dominated groups contained 30 members. In Table 1, we list the groups in the sample along with their redshift and the X-ray properties measured by OP04 used in this work.

2.2 Identifying radio sources

We then divided the elliptical-dominated groups into radio-loud and radio-quiet subsamples based on the properties of any radio source associated with each group. For each group in the sample, we used NED, NVSS (Condon et al. 1998) and FIRST (Becker et al. 1995) to locate radio sources that could potentially be associated with a group member. We first checked NED for any known radio galaxies associated with the group’s galaxies. If an associated radio source was found, we adopted the 1.4-GHz radio flux from the NED database. For any groups where a radio source was not found in this way, we searched for sources within a radius of 10 arcmin using NVSS and FIRST. We then checked the location of each candidate for an associated radio source on the DSS2 optical images to ensure that the radio source was roughly at the centre of a group galaxy (using SIMBAD to confirm that the galaxy is at the redshift of the group). If this was not the case, then we rejected the radio source on the basis that it was probably a background object. This method should be a more robust way of defining radio-loud and radio-quiet groups than the method we used in Croston et al. (2003), as the latter may contain spurious “radio-loud” designations if any of the radio sources were not in fact associated with the group. Table 2 gives the 1.4-GHz radio flux and luminosity densities, $L_{1.4}$, and the location for all of the associated sources. We also list the distance between the radio source and group centre, defined in OP04 as the position of the group-member galaxy nearest to the centroid of the X-ray emission. In two cases (NGC 5171 and HCG 90) the radio source is a significant distance from the group centre, which may reduce the likelihood that it could strongly affect the group gas properties; however, as in both cases the radio-source is clearly associated with a group galaxy and lies in the extended X-

¹ <http://www.eso.org/dss>

Table 1. The elliptical-dominated groups sample. Properties listed here are taken from OP04. -model parameters marked with a star are estimated using the method described in the text.

Group	Redshift	Temperature (keV)		Abundance (Z)		$\log(L_X \text{ ergs}^{-1})$		r_{cut} (kpc)	r_c (kpc)	
HCG 42	0.0128	0.75	0.04	0.29	0.10	41.99	0.02	112	0.56	4.69
HCG 62	0.0146	1.43	0.08	2.00	0.56	43.14	0.04	282	0.48	2.44
HCG 90	0.00880	0.46	0.06	0.08	0.03	41.49	0.05	101	0.41	0.91
HCG 97	0.0218	0.82	0.06	0.23	0.10	42.37	0.05	339	0.44	2.73
NGC 383	0.0173	1.51	0.06	0.42	0.08	43.07	0.01	633	0.36	2.11
NGC 524	0.00793	0.65	0.07	0.22	0.15	41.05	0.05	56	0.45*	0.37*
NGC 533	0.0181	1.08	0.05	0.68	0.23	42.67	0.03	372	0.42	2.21
NGC 720	0.00587	0.52	0.03	0.18	0.02	41.20	0.02	65	0.47	1.15
NGC 741	0.0179	1.21	0.09	2.00	0.67	42.44	0.06	386	0.44	2.30
NGC 1052	0.00492	0.41	0.15	0.00	0.02	40.08	0.15	25	0.45*	0.04*
NGC 1407	0.00565	1.02	0.04	0.23	0.05	41.69	0.02	105	0.46	0.08
NGC 1587	0.0122	0.96	0.17	0.47	1.24	41.18	0.09	77	0.46	4.34
NGC 3557	0.00878	0.24	0.02	0.00	0.01	42.04	0.04	95	0.52	1.13
NGC 3665	0.00692	0.47	0.10	0.17	0.14	41.11	0.08	71	0.47	1.08
NGC 3607	0.00411	0.35	0.04	0.23	0.10	41.05	0.05	62	0.39	1.98
NGC 3923	0.00459	0.52	0.03	0.18	0.05	40.98	0.02	34	0.55	0.63
NGC 4065	0.0235	1.22	0.08	0.97	0.48	42.64	0.05	425	0.36	3.08
NGC 4073	0.0204	1.52	0.09	0.70	0.15	43.41	0.02	470	0.43	9.42
NGC 4261	0.00785	1.30	0.07	1.23	0.42	41.92	0.03	112	0.44	40.08
NGC 4636	0.00565	0.84	0.02	0.41	0.05	41.49	0.02	68	0.47	0.30
NGC 4325	0.0252	0.82	0.02	0.50	0.08	43.15	0.01	307	0.58	27.56
NGC 4589	0.00676	0.60	0.07	0.08	0.03	41.61	0.05	122	0.52	9.33
NGC 4697	0.00454	0.32	0.03	0.07	0.02	41.01	0.02	53	0.46	1.25
NGC 5044	0.00820	1.21	0.02	0.69	0.06	43.01	0.01	180	0.51	5.96
NGC 5129	0.0232	0.84	0.06	0.66	0.28	42.33	0.04	151	0.43	3.14
NGC 5171	0.0232	1.07	0.09	1.47	1.25	42.38	0.06	298	0.45*	81.26
NGC 5322	0.00702	0.23	0.07	0.00	0.02	40.71	0.10	43	0.45*	0.18
NGC 5846	0.0063	0.73	0.02	1.25	0.69	41.90	0.02	94	0.51	2.19
NGC 5930	0.00969	0.97	0.27	0.17	0.12	40.73	0.07	29	0.45*	0.19*
IC 1459	0.00569	0.39	0.04	0.04	0.01	41.28	0.04	121	0.45	0.74

Table 2. Radio sources associated with groups. Coordinates are for the radio-source position. Column 3 (D) is the physical distance between the radio source and the group centre (see text for discussion). Luminosity densities are determined by assuming that the source is at the redshift of the group.

Group	RA (J2000)	Dec (J2000)	D /kpc	$F_{1.4}/\text{Jy}$	$L_{1.4}/\text{WHz}^{-1}$	Ref
NGC 383	01 07 24.9	+32 24 45	5.0	0	3.4×10^4	NED
NGC 524	01 24 47.7	+09 32 21.7	0.51	0.0035	5.4×10^0	NVSS
NGC 533	01 25 31.3	+01 45 33	0	0.0291	2.2×10^2	NED
NGC 741	01 56 22.1	+05 37 39.8	6.2	1.0	7.2×10^3	NVSS
NGC 1052	02 41 04.8	-08 15 21.1	0.01	0.913	5.1×10^2	NVSS
NGC 1407	03 40 11.9	-18 34 49.0	0.20	0.0877	6.8×10^1	NVSS
NGC 1587	04 30 39.9	+00 39 42.1	0.22	0.123	4.1×10^2	NVSS
NGC 3557	11 09 57.7	-37 32 20.7	0.91	0.484	1.6×10^3	NVSS
NGC 3607	11 17 01.6	+18 08 44.8	30.0	0.0181	6.4×10^0	NVSS
NGC 3665	11 24 43.4	+38 45 44	0	0.113	1.2×10^2	NED
NGC 3923	11 51 05.0	-28 46 10.5	2.3	0.0312	1.7×10^1	NVSS
NGC 4261	12 19 23.2	+05 49 31	0	18.0	2.0×10^4	NED
NGC 4636	12 42 50.3	+02 41 18.7	0.64	0.299	1.3×10^2	NVSS
NGC 5044	13 15 24.0	-16 23 7.6	0.27	0.0347	5.0×10^1	NVSS
NGC 5171	13 29 47.9	+11 42 33.8	186	0.025	3.1×10^2	NVSS
NGC 5930	15 26 06.7	+41 40 21.0	3.7	0.108	1.9×10^2	NVSS
HCG 62	12 53 05.6	-09 12 21	1.7	0.0049	1.6×10^1	NVSS
HCG 90	22 02 02.0	-31 52 10.5	81	0.0368	1.4×10^3	NVSS
IC 1459	22 57 10.7	-36 27 43.0	0.19	1.28	9.1×10^2	NVSS

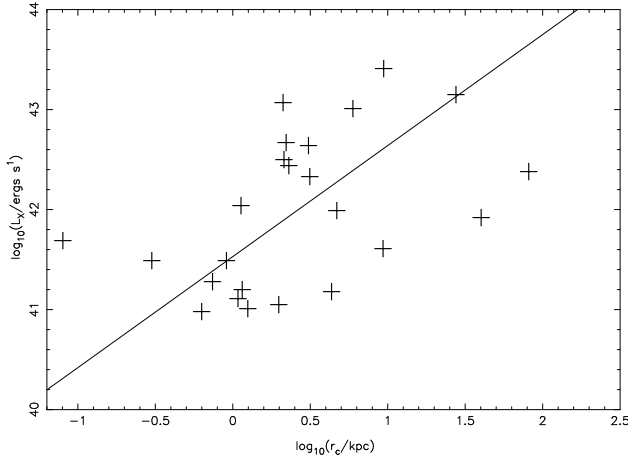


Figure 1. Plot of $\log(L_X)$ vs. $\log(r_c)$, illustrating the trend between these quantities. The OLS bisector fit to this line is overplotted and has a slope of 1.11 and an intercept of 41.53 at $\log_{10}(r_c) = 0$. We used this relation to estimate r_c for the groups where OP04 were unable to measure r_c -model parameters.

ray halo detected with *ROSAT*, we include these two radio sources in the sample.

In our earlier analysis (Croston et al. 2003), we chose a single cut-off to discriminate between radio-quiet and radio-loud groups. However, at lower luminosities it is difficult to distinguish between AGN-related radio emission and emission from other processes, such as starbursts. The radio source population is dominated by starbursts at 1.4-GHz luminosities below $10^{23} \text{ W Hz}^{-1}$ (Sadler et al. 2002). All of the radio source identifications are with elliptical galaxies, so that a starburst origin is unlikely, and the majority of the sources have also been previously identified as AGN. However, we may detect weak AGN emission in elliptical galaxies that have never had a radio source sufficiently powerful to have affected the group properties. We therefore tested the importance of the radio-luminosity cut-off, by carrying out all of the analysis that follows for three choices. We first used a cut-off (c_0) of $L_{1.4}^{\text{cut}} = 0$, so that the possession of *any* radio source above the NVSS flux density limit meant that a group was considered to be radio-loud. We then chose two higher cut-offs, based on the luminosity density of NGC 3665, a comparatively weak double-lobed radio galaxy, as in the analysis of Croston et al. (2003). These cut-offs (c_1 and c_2) are $L_{1.4}^{\text{cut}} = 1.2 \times 10^{21} \text{ W Hz}^{-1}$ ($L_{\text{NGC 3665}}=10$) and $L_{1.4}^{\text{cut}} = 6 \times 10^{21} \text{ W Hz}^{-1}$ ($L_{\text{NGC 3665}}/2$). Table 3 gives the total number of groups in each subsample for the three choices of radio-luminosity cut-off. We note that the NVSS flux limit of 2.3 mJy may introduce some bias into the selections, as this corresponds to a limiting luminosity of $3 \times 10^{21} \text{ W Hz}^{-1}$ for the highest redshift group, NGC 4325, at $z = 0.0252$. This limit is close to the cut-off luminosities, so that for cut-offs c_0 and c_1 a few high-redshift groups could have been incorrectly classed as radio-quiet despite possessing a radio-source more luminous than the cut-off luminosity. There are five groups with sufficiently high redshift that a radio source more luminous than c_1 could have been missed. However, a radio source of luminosity $> c_2$ would be detectable in all of the groups, so that the results for this cut-off should provide a check for whether this bias is important.

2.3 Radio sources in the OP04 parent population groups

We found a surprisingly high fraction of radio sources in the sample of elliptical-dominated groups from the OP04 catalogue (19/30 = 63 per cent, assuming cut-off c_0). It is often stated that radio galaxies are not common; a small fraction of elliptical galaxies [e.g. 5 per cent, Schmidt (1978)] host a large radio galaxy. However, the fraction is certainly higher for the brightest ellipticals (e.g. Birkinshaw and Davies 1985), and Ho (1999) discusses the recent detections of small radio cores in many nearby elliptical galaxies, concluding that these are likely to be low-luminosity AGN. Since the preferred environment of radio galaxies may be the centres of elliptical-dominated groups or poor clusters (e.g. Best 2004), the high fraction of “radio-loud” groups in the sample may not be unexpected. If radio galaxies are found in such a high fraction of this type of group, then our results will have important implications for the properties and evolution of groups. For this reason, it is crucial to test whether or not the OP04 X-ray observed sample of groups may be biased in its radio properties. The OP04 sample was chosen by merging nine catalogues of optical groups and then cross-correlating the resulting list with the *ROSAT* observing log. The parent catalogue is unbiased with respect to the groups’ radio properties; however, it is possible that the *ROSAT* archive contains a high fraction of groups with active galaxies, since *ROSAT* observed many radio galaxies. This could bias the OP04 sample towards groups containing radio galaxies, although groups with previously known radio galaxies make up a fairly small fraction of the OP04 sample.

To test whether the fraction of radio-loud groups in our sample is biased, we looked at the parent catalogues used by OP04. As we were only interested in the properties of elliptical-dominated groups, we wanted to use an electronically available catalogue that contained information about the morphology of the dominant galaxy in each group. The whole-sky group catalogue of Garcia (1993), taken from the Lyon-Meudon Extragalactic Database fits these criteria. It contains 485 groups having $z < 0.02$. This sample is large enough that we can test whether its radio properties are consistent with those of the OP04 sample.

Using Vizier², we extracted from the Garcia catalogue all groups whose dominant galaxy has type E (elliptical) or L (S0) (these classifications are taken from de Vaucouleurs et al. 1991). Although we excluded groups with a dominant galaxy with a convincing S0 designation in our sample definition, we decided to include them here, for two reasons. Firstly, as mentioned earlier, we found several dominant galaxies in our sample with S0 designations where later work revealed them to be misclassified ellipticals. Secondly, a surprisingly low fraction of the groups in the sample had “E” designations, so that the test sample would have been quite small. Including all the S0 groups means that the resulting radio-loud fraction will be a conservative lower limit, as many of the S0 identifications will be correct. The final sample of E and S0 groups from the Garcia sample contains 135 groups (30 per cent of the original sample).

We then cross-correlated the Garcia E and S0 groups with NVSS, searching for radio sources within 15 arcsec of the centre of the dominant galaxy. This method is not as accurate as the method we used for the OP04 radio identifications; however, the more detailed method is too cumbersome for this larger sample. To ensure a fair comparison, we carried out the same cross-correlation for our

² <http://vizier.u-strasbg.fr/>

Table 3. Samples sizes for different choices of radio-luminosity cut-off, $L_{1.4}^{\text{cut}}$ as given in the text.

Cut-off number	$L_{1.4}/\text{WHz}^{-1}$	Number in RQ sample	Number in RL sample
c0	0	11	19
c1	1.2×10^{21}	13	17
c2	6×10^{21}	16	14

elliptical-dominated groups sample, using the coordinates given in OP04.

For the E/S0 Garcia subsample, we found radio sources associated with 41 groups. 32 groups had coordinates outside the region covered by NVSS, so that the final “radio-loud” fraction of the Garcia subsample is 41/103, or 39.8 per cent. For our elliptical-dominated sample (Table 1), using the same method, we found a “radio-loud” fraction of 16/30, or 53.3 percent. Therefore the “radio-loud” fraction of the elliptical-dominated groups in OP04 is consistent with that in this parent catalogue. The fraction we obtained here for our OP04 subsample is slightly lower than that obtained using the more accurate identification method described in Section 2.2, which was 19/30, or 63 percent. This is unsurprising, as the detailed method would find sources associated with *any* large elliptical in the group, whereas this cross-correlation method will only find sources associated with the dominant galaxy.

We conclude that the OP04 group sample is not excessively biased with respect to the groups’ radio properties. The true fraction of elliptical-dominated groups with radio sources may be 40–50 percent (since our result for the Garcia sample is a conservative lower limit), rather than being as high as is suggested by our original analysis of the OP04 sample. It is interesting that such a high fraction of elliptical-dominated groups is likely to possess an AGN-related radio source. If all elliptical-dominated groups are capable of hosting radio sources, this result could indicate that radio galaxies have a high duty cycle. Radio sources with obvious double-lobed structure make up roughly half of the radio sources in the sample, so that perhaps only half of the 40–50 percent of elliptical-dominated groups with radio sources could be considered to be in a very active state. Nonetheless, this suggests that a duty cycle where every elliptical-dominated group contains a radio source that is active for 1/4 of the time. Weaker sources with no detected double-lobed structure may be in a less active stage, and the groups with no radio source above the NVSS limit may be in the least active phase. If this model is correct, then the effects of radio sources are likely to be important at some level in all elliptical-dominated groups. The analysis of the Garcia sample found that E/S0-dominated groups made up 30 percent of the sample. Although this is a minority of groups, E/S0-dominated groups are more likely to host a group-scale X-ray atmosphere (Osmond and Ponman 2004). They are therefore likely to be in a more relaxed state, so that their X-ray properties will be of more relevance to structure-formation models.

2.4 Issues with X-ray luminosity comparisons

The analysis we carried out in Croston et al. (2003) is based on the $L_X = T_X$ relations for radio-loud and radio-quiet groups. In that analysis we did not take into account the choice of radius to which the X-ray luminosity was measured. OP04 used an X-ray extraction radius defined by the extent of X-ray emission at a significant level above the background. They then used the luminosities obtained

for these regions and their fitted β -model parameters to extrapolate the luminosity to a fixed overdensity radius, r_{500} (= the radius corresponding to 500 times the critical density of the Universe). We were concerned that the choice of radius used for the luminosity determination might affect the results. There are problems in this context with both radii used by OP04. A cut-off radius defined by the extent of X-ray emission biases the X-ray luminosity-temperature ($L_X = T_X$) relation in the sense that a smaller fraction of the atmosphere will be measured for fainter groups, because the surface brightness drops below the background at a smaller radius. However, choosing a cut-off at r_{500} may not be suitable for our analysis either, as the method used by OP04 to define r_{500} is temperature-dependent, so that the luminosity is measured to a larger physical radius for hotter groups. If groups have been heated by the presence of a radio source, the choice of r_{500} will have the effect of reducing the significance of any heating effect we measure.

Clearly, it would be preferable to use the luminosity integrated out to infinity. Unfortunately this is not possible using a β -model representation of the groups, as the solid angle integral of the surface brightness diverges for values of $\beta = 2$, so that a cut-off radius must be used for the luminosity extrapolation. As neither of the two choices of radius used by OP04 is entirely unbiased, we performed the $L_X = T_X$ analysis for four choices of luminosity cut-off radius. These were: the *ROSAT* extraction radius, r_{cut} , as given in Table 1; the fixed over-density radius, r_{500} , as calculated by OP04; a physical radius of 200 kpc, r_{phys} ; and r_{core} , defined as 4 times the group core radius, r_c . We used the luminosity measured to r_{cut} and the fitted β -model parameters to calculate the luminosity to r_{500} , r_{phys} and r_{core} . We neglected the axial ratio parameter, e , included in the OP04 fits, which means that the extrapolated luminosities will be slightly overestimated for groups that have a large axial ratio. The maximum value of e for a source in our sample is 2.65 (NGC 4589), but most e values are in the range of 1.0–1.5. The radio-loud and radio-quiet groups have similar distributions of e , and so our conclusions should not be affected. OP04 could not fit a β model for five sources, and for these we used $\beta = 0.45$ (the median value measured for the sample) and r_c determined by using the rough correlation between X-ray luminosity and r_c shown in Fig. 1 - $L_X = 2.9 \times 10^{41} (r_c/\text{kpc})^{1.11} \text{ ergs s}^{-1}$.

Another consideration is whether the measured X-ray luminosities contain any contribution from sources other than the group gas, i.e. from AGN and X-ray binaries. *Chandra* observations can resolve the X-ray binary population and allow the integrated luminosity from X-ray binaries to be determined. Kraft et al. (2001) find an integrated X-ray luminosity of $5 \times 10^{39} \text{ ergs s}^{-1}$ for the population of X-ray binaries in Centaurus A. Zhang and Xu (2004) examine the X-ray binary population in NGC 1407, one of the groups in the sample, which has a comparatively prominent X-ray binary population, and find that resolved X-ray binaries account for < 20 percent of the galaxy-scale extended X-ray emission detected with *Chandra* (or $1.5 \times 10^{40} \text{ ergs s}^{-1}$, only 3 per

cent of the *ROSAT*-measured L_X for the group-scale emission from NGC 1407). We conclude that contamination from X-ray binaries is not important to our results. Any contamination from X-ray binary emission that cannot be resolved by *Chandra* should affect the radio-quiet and radio-loud groups in the same way. We discuss the issue of AGN contamination in Section 3.1.

2.5 $L_X = T_X$ relations

For each of the 12 combinations of radio and radius cut-offs, we fitted an $L_X = T_X$ relation to the radio-quiet and radio-loud subsamples. Using the temperature measurements of OP04 and the luminosities determined as described above, we fitted the OLS (ordinary least squares) bisector (Isobe et al. 1990) to each dataset for consistency with OP04. Table 4 gives the parameters for the resulting fits. We plot L_X vs. T_X for each radio cut-off in Fig. 2 (showing only the results for r_{cut}) with the best-fitting radio-quiet relation overplotted. There is a clear tendency for radio-loud groups to be on the hotter side of the radio-quiet relation for all combinations of radio cut-off and luminosity extraction radius. (One major exception to this trend is NGC 3557, a radio-loud group that is much cooler than the prediction for its luminosity, but this may be due to including the cooler galaxy atmospheres of group members, which are prominent in a *Chandra* observation.)

We tested the significance of the trends illustrated in Fig. 2 for each choice of luminosity cut-off. We transformed the luminosity values into a predicted temperature using the appropriate best-fitting radio-quiet $L_X = T_X$ relation, as given in Table 4. We then rotated the coordinate system by 45 degrees so that the x -coordinate in temperature corresponds to perpendicular distance from the best-fitting line. We then performed a 1-D Kolmogorov-Smirnov test comparing the distributions of x (perpendicular distance from the line) for the radio-quiet and radio-loud samples of each case. The results are given in Table 4. In all but two cases, the probability that the two subsamples have the same parent population is < 10 percent, and in more than half of the remaining cases, the probability is less than < 5 percent.

We therefore conclude that there is good evidence that radio-loud and radio-quiet groups display different gas properties. The choice of radio-luminosity cut-off does not appear to have an important effect, whereas the choice of X-ray luminosity radius is crucial. To obtain a more consistent set of X-ray luminosity and temperature measurements, higher sensitivity data would be required so that the temperature and luminosity could be measured to much larger radii, and the need for extrapolation would be reduced.

3 INTERPRETATION OF THE RESULTS

The gas properties of radio-loud and radio-quiet groups differ in the sense that radio-loud groups of a given luminosity are likely to be hotter than the radio-quiet groups. There are several possible explanations for this result, which we examine in this section.

The first question is whether contamination from AGN emission could have affected the results for radio-loud groups. We test this in Section 3.1. We then consider three possible physical origins for the difference in the properties of radio-loud and radio-quiet groups: radio-source heating (Model I), a luminosity deficit caused by the radio source (Model II), or an external mechanism that is triggering the radio source *and* heating the gas (Model III). Models I and II are related, since any temperature increase would lead to an increase in pressure, expansion and a subsequent decrease in

density on timescales determined by the sound speed; however, as a first step in understanding the radio-source impact, it is important to test whether the primary effect seen in our results comes from an increase in the group temperature or a decrease in X-ray luminosity. In Section 3.2 we test Model I (radio-source heating), by examining whether there is any evidence that the strength of the inferred heating of radio-loud groups correlates with the properties of the radio sources. In Sections 3.3 and 3.4, we carry out two investigations to test Model II (a radio-source-induced luminosity decrement). Firstly, we examine the distribution of gas, parametrised by the β -model, to determine whether this differs for radio-quiet and radio-loud groups. We then examine the correlation between L_X and optical luminosity to see whether the X-ray luminosities of radio-loud groups are lower relative to their optical luminosities than is the case for radio-quiet groups, as would be expected in the second model. In Section 3.5, we test Model III (an external mechanism), by examining the optical properties of the two subsamples to find out whether the radio-loud groups could be in a specific evolutionary state, different to that of the radio-quiet groups, where the triggering of radio sources *and* the heating of gas might be favoured. Finally, in Section 3.6 we present a study of archive *Chandra* observations of the radio-loud groups to look for further evidence of radio-source heating and interactions between the radio source and group gas.

3.1 AGN contamination and the reliability of the OP04 results

OP04 state that they have taken into consideration any contribution from a central AGN to the X-ray emission via their point-source exclusion method. Central AGN were excluded in 22 cases (Osmond, private communication); however, this does not include all of the radio-loud groups in our sample. Contamination from strong non-thermal emission might result in higher fitted gas temperatures, which could shift groups with AGN on the $L_X = T_X$ plane. However, if there were a large contribution from AGN-related X-ray emission, then the measured X-ray luminosity from the group gas would be overestimated; this would act in the opposite sense. It is therefore essential to check that AGN contamination is not leading to spuriously high temperatures or overestimation of the group luminosities, and so we felt it necessary to confirm the results of OP04 for several radio-loud groups. In addition, as our results rely strongly on the accuracy of OP04's *ROSAT* analysis, we felt it was appropriate to independently measure the temperature and luminosity of 3 radio-loud groups, to test for AGN contamination, and 3 radio-quiet groups, to confirm the reliability of the luminosity and temperature measurements.

From the *XMM* analysis of Croston et al. (2003), we found that the AGN in 3C 66B and 3C 449 (which are more powerful than most of the radio sources in the sample we use here) would not significantly contaminate the spectral measurements for the group atmospheres. The measured temperatures and luminosities in our sample are therefore likely to be reliable for groups with $L_X > 10^{42} \text{ erg s}^{-1}$. For this reason, we selected three groups with lower X-ray luminosities: NGC 4261, NGC 1407, where OP04 did not exclude the central AGN, and HCG 90.

In order to test the influence of AGN contamination, we extracted a spectrum for the extraction region used by OP04 (a circle of radius r_{cut}), but excluding the central two arcminutes, so as to ensure that the majority of the AGN emission was excluded. We used a surrounding annulus for background and excluded any contaminating point sources by eye. Our analysis is therefore sig-

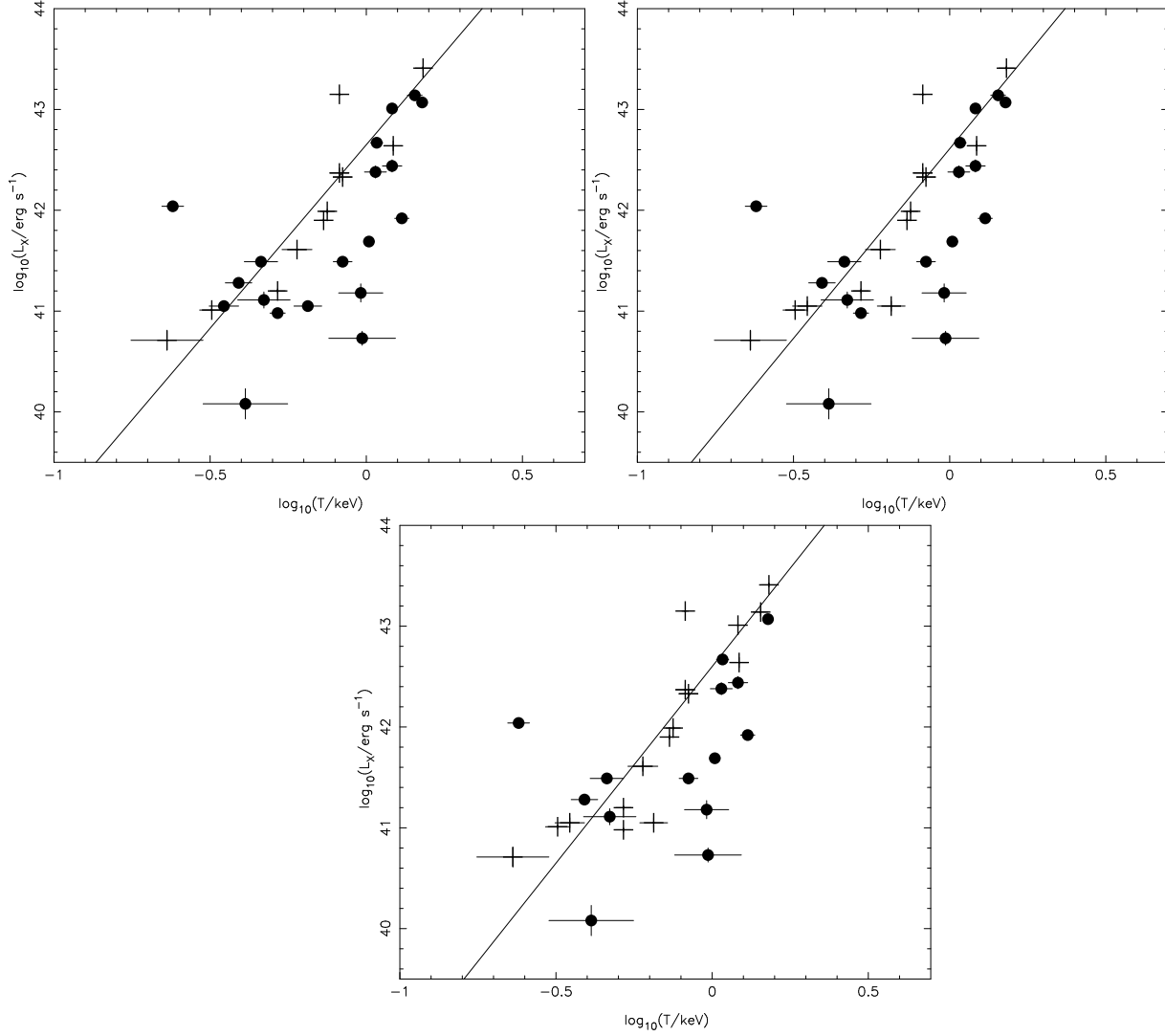


Figure 2. $L_X = T_X$ plots for r_{cut} , top left for c0, top right c1, and bottom c2. Overplotted are the best-fitting radio-quiet relations for each set. + symbols are radio-quiet groups and filled circles are radio-loud groups.

Table 4. K-S test results and best-fitting slopes and intercepts for the L_X / T_X relations as described in the text. D is the K-S statistic for the given pair of radio-quiet and radio-loud samples, and Prob is the null hypothesis probability for obtaining the given value of D .

Dataset	c0				c1				c2			
	Slope	Intercept	D	Prob	Slope	Intercept	D	Prob	Slope	Intercept	D	Prob
r_{cut} (RL)	3.30 0:86	42.15 0:15	0.488	0.048	3.33 0:86	42.16 0:15	0.416	0.114	2.75 0:71	42.03 0:18	0.464	0.054
r_{cut} (RQ)	3.64 0:61	42.65 0:14			3.76 0:72	42.61 0:14			3.90 0:81	42.60 0:10		
r_{500} (RL)	3.07 0:72	42.35 0:12	0.488	0.048	3.19 0:73	42.35 0:12	0.434	0.088	2.65 0:59	42.24 0:14	0.517	0.022
r_{500} (RQ)	3.36 0:51	42.77 0:12			3.37 0:57	42.73 0:13			3.58 0:70	42.73 0:09		
r_{phys} (RL)	2.76 0:72	42.15 0:12	0.488	0.048	2.84 0:72	42.15 0:13	0.452	0.068	2.22 0:51	42.01 0:12	0.536	0.016
r_{phys} (RQ)	3.05 0:50	42.57 0:15			3.08 0:56	42.54 0:15			3.34 0:65	42.56 0:10		
$r_{4\text{core}}$ (RL)	3.42 1:10	41.47 0:18	0.450	0.084	3.40 1:08	41.49 0:19	0.416	0.114	2.68 0:91	41.29 0:20	0.518	0.022
$r_{4\text{core}}$ (RQ)	3.83 0:77	42.07 0:26			4.02 0:94	42.02 0:26			4.13 1:04	42.04 0:18		

nificantly cruder than that of OP04, who carried out a more complicated background estimation and performed good-time interval analysis. In all cases our measured temperature is the same within the (1 %) errors. However, the measured luminosities in two cases are significantly lower than the OP04 results. We conclude that

there is no risk that the observed difference in the temperature distribution of radio-quiet and radio-loud groups is due to spuriously high temperatures as a result of AGN contamination. The lower luminosity for NGC 4261 is likely to be due to our larger AGN exclusion region (which must include significant group emission).

In the case of NGC 1407, the slightly lower luminosity is likely to be because OP04 did not exclude the AGN. If the AGN contributes some of the measured luminosity in a few sources, then the OP04 luminosity measurements for some of the radio-loud groups may be slightly overestimated, which would mean that the significance of the effect we observe is underestimated. If the true errors on temperature for these groups are slightly larger than those given by OP04, this would not have any effect on the K-S test results and our conclusions. Finally, since OP04 excluded the AGN in the poorest radio-loud groups, including NGC 1052 and IC 1459, we conclude that AGN contamination is unlikely to be a problem for our results.

Even if the AGN emission does not significantly affect the measured temperature, it can have a more important effect on the surface brightness profile. OP04’s neglect of an AGN may affect the fitted β -model parameters for a few groups. Several of the most powerful radio galaxies in the sample (e.g. NGC 383, from which the AGN was not removed, and NGC 4261) are among the groups fitted with a second central β -model. It is possible that these inner β -models are, in fact, principally modelling the point-source emission from the central AGN, although there is also evidence for a galaxy atmosphere in NGC 383 (Hardcastle et al. 2002). Since an AGN component would be modelled out in this way, the β -model parameters for the extended emission should be reliable. That a second β -model was not required for many of the radio-loud groups, in combination with the lack of any effect on the measured temperatures, supports the conclusion that for most of the less powerful radio sources the AGN contribution to the X-ray emission is not significant.

The radio-quiet groups chosen to check the reliability of the OP04 results were selected to cover a wide range in X-ray luminosity and temperature. They are NGC 97, NGC 720, and NGC 4325. For each group, we extracted a spectrum using the extraction region of OP04 (a circle of radius r_{cut}) using the same background and point-source identification methods as above, and fitted a *mekal* model with free abundance to determine the temperature and X-ray flux of the group atmosphere. In all cases the results are in good agreement with those of OP04, so we conclude that the OP04 luminosity and temperature determinations are reliable both for radio-quiet and radio-loud groups.

3.2 Testing Model I: correlations with radio luminosity

The results presented in Section 2 strongly suggest that radio galaxies are having an important effect on the properties of the surrounding group gas. We therefore decided to investigate whether there is any relationship between the observed “temperature excesses” and the radio properties of the associated sources, as would be expected in a radio-source heating model. In the following analysis, we use only the results for radio-luminosity cut-off >0 so as to include the widest range of radio powers.

We used the 1.4-GHz radio luminosity density (Table 2) as a measure of the amount of energy a given source might be able to provide. Radio luminosity is not an ideal indicator of radio source energy input, as the amount of energy transferred from the expanding radio plasma to the surrounding gas depends on several factors, such as source size and age, which are in many cases unknown. The size of the source depends on its angle to the line of sight, which is usually poorly constrained. The source’s age, which is also required to estimate the total energy input, is even more difficult to determine. Indeed, a few of the radio sources in the sample are unresolved with NVSS and FIRST, and do not have identifiable double-lobed structure. However, low-frequency radio luminosity

should trace the jet kinetic luminosity reasonably well, so that in the absence of useful information on the sizes and ages of all of the sources, the 1.4-GHz luminosity is the best measure of energy input available.

We first compared the radio luminosity with T , the difference between the measured temperature and that predicted by the appropriate $L_X = T_X$ relation. Table 5 gives the results of Spearman rank correlation tests for each choice of X-ray luminosity radius. For the Spearman test, groups with no temperature increase were assigned $T = 0$: this applies to 5/19 groups for r_{cut} and r_{500} , 6/19 for r_{phys} , and 3/19 for r_{core} . In all cases there is little evidence for a correlation. This is perhaps unsurprising, because the observed temperature increase produced by a radio galaxy of given luminosity should depend not only on the unknown properties of the radio source, as mentioned above, but also on the heat capacity of the group gas being heated. A similar analysis using the fractional temperature change, $T = T$, did not give an improved correlation.

We therefore estimated the heat capacity of each group’s environment using the spectral and spatial properties of the X-ray emission given by OP04. The heat capacity is $C = (3/2)Nk$, where N is the total number of particles, obtained by integrating over the density profile using the best-fitting β -model parameters, with a central proton density obtained from the X-ray luminosity and best-fitting *mekal* model parameters.

To study the relationship between the observed “heating” and radio luminosity, we examined the correlation between E_{req} , the energy required to heat the gas in a given group from the predicted temperature to the measured temperature ($C - T$), and $L_{1:4}$. The heat capacities were calculated separately for each of the four choices of limiting radius. Fig. 3 shows the relationship between $L_{1:4}$ and E_{req} for each choice of r . For groups with no temperature excess, we calculated an upper limit to the energy input by determining the amount of energy that would be required to shift the group significantly to the ‘hotter’ side of the appropriate $L_X = T_X$ relation. As the sample includes upper limits, we used survival analysis techniques to determine the generalised Kendall’s correlation coefficient using ASURV (Lavalley et al. 1992). Table 5 contains the results of the correlation analysis for each case. There is a less than 5 percent probability of obtaining the measured value of E_{req} by chance for 2 out of 4 cases. The high value of 14 per cent for r_{core} is probably because in many cases r_{core} is physically small compared to the other choices for r , so that the heat capacity does not include much of the gas. For all four choices of radius, there is a stronger correlation here than was found for T alone.

Since the calculated heat capacity is related to the measured X-ray luminosity, we were concerned that the correlation between $L_{1:4}$ and E_{req} could be caused by an $L_X = L_{1:4}$ correlation due to the flux limits in the X-ray and radio samples. We therefore also carried out Spearman rank tests to look for a correlation between heat capacity and $L_{1:4}$. Those results are also included in Table 5, and show that the correlation between $L_{1:4}$ and heat capacity is much weaker than that with E_{req} in all cases.

The presence of a correlation (albeit with a large scatter) between radio luminosity and the energy input needed to cause the observed temperature increase provides support for a model where the temperature increase is due to radio-source heating. The large scatter is not surprising, given the many unknown factors, such as source size and age, that would affect the amount of observed heating.

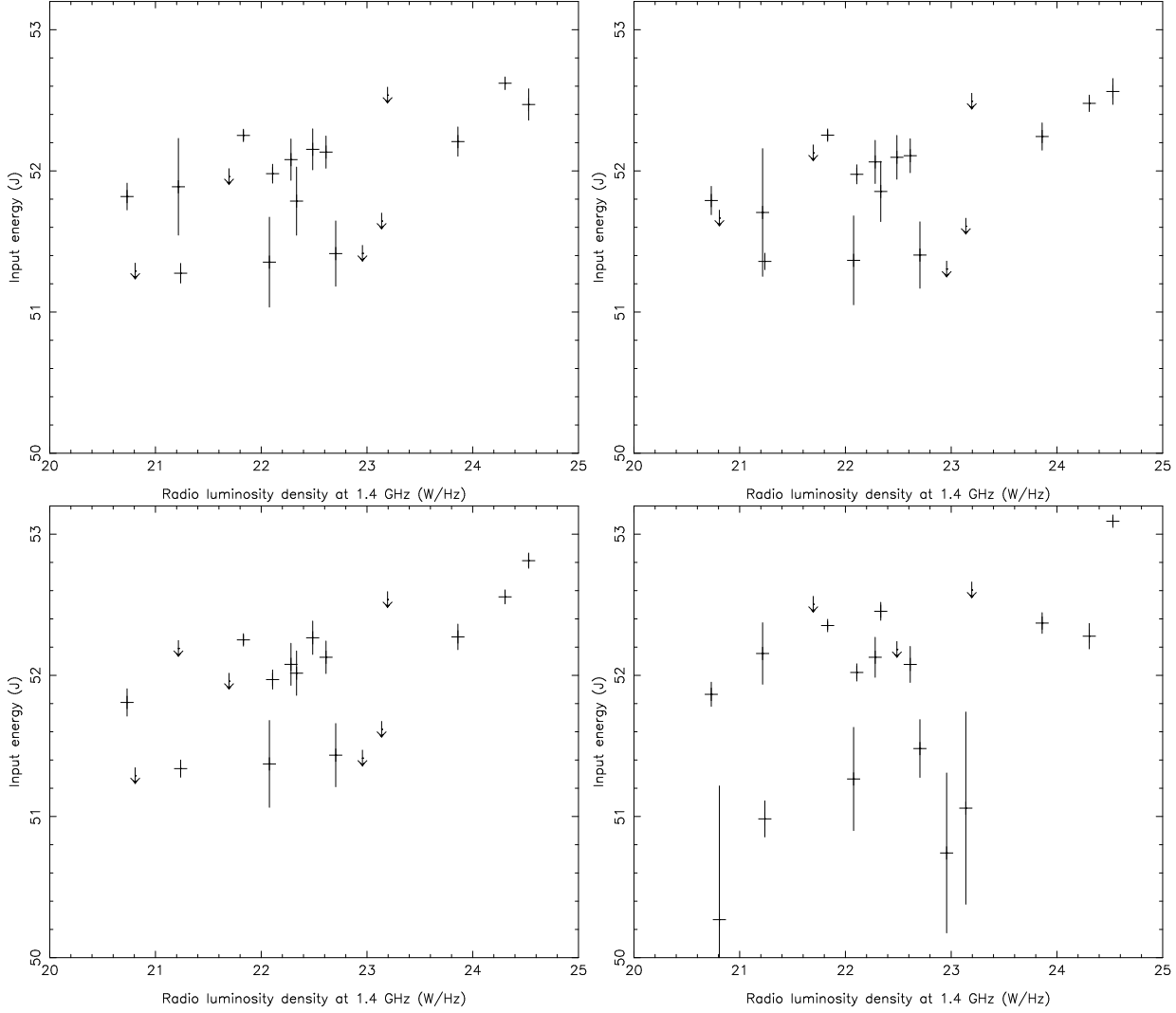


Figure 3. Plot of $L_{1.4}$, the 1.4-GHz radio luminosity, vs. E_{req} , the necessary heat in put to produce the temperature increase, for r_{cut} (top left), r_{500} (top right), r_{phys} (bottom left) and $r_{4\text{core}}$ (bottom right). + symbols are groups with temperature excesses; arrows indicate upper limits for groups with no observed excess, calculated as described in the text.

Table 5. Results of correlation analysis for $L_{1.4}$ and T , E_{req} and C . The sample contains 19 groups, so for all of the tests there are 17 degrees of freedom.

Dataset	T		E_{req}		C	
	r_s	Probability	Kendall's	Probability	r_s	Probability
r_{cut}	0.184	0.450	1.992	0.046	0.312	0.193
r_{500}	0.214	0.379	1.921	0.055	0.325	0.175
r_{phys}	0.369	0.121	2.555	0.011	0.312	0.193
$r_{4\text{core}}$	0.168	0.491	1.472	0.141	0.314	0.190

3.3 Testing Model II: -model properties

We studied the -model properties of the radio-quiet and radio-loud groups to determine whether the spatial distribution of gas is affected by the presence of a radio source. We compared three parameters, f_{fit} , the fitted value of β from OP04, f_{spec} , the spectroscopic value of β from OP04, and $R = f_{\text{spec}} - f_{\text{fit}}$. For each of these properties, we compared the values for the radio-quiet and radio-loud subsamples for radio cut-off c_0 . We performed a 1-D

K-S test to determine whether the “radio-quiet” and “radio-loud” subsamples differed in each case. Fig. 4 shows histograms of the distributions of f_{fit} , f_{spec} , and R for the radio-quiet and radio-loud samples.

There is no evidence that the parent population differs significantly for any of the three parameters. Since the f_{spec} have large errors, using the K-S test to compare the two samples may not be very reliable. We also used a median test to compare the two samples, and find a low probability that the distributions of f_{fit} have a

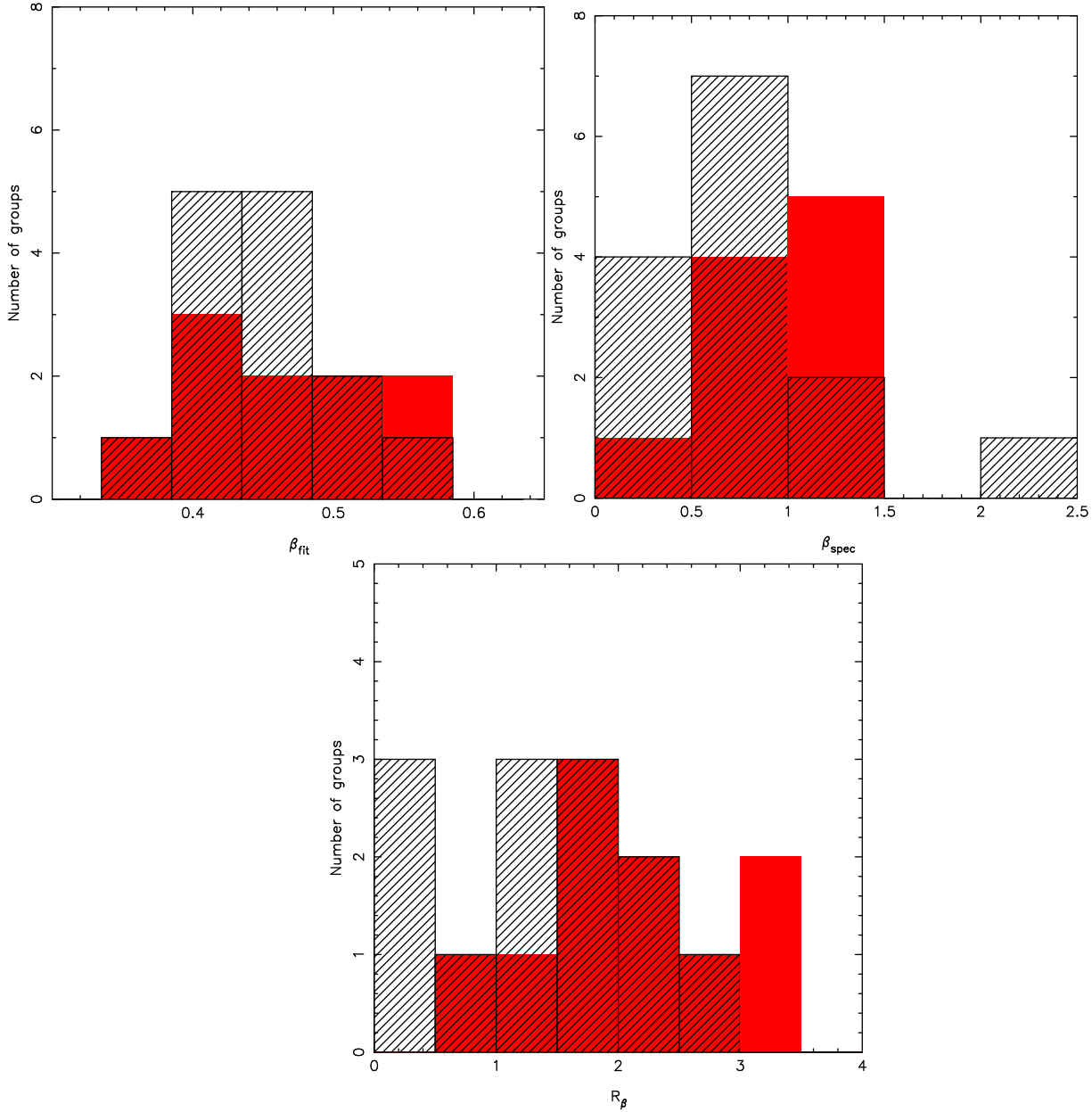


Figure 4. Histograms showing the distribution of β_{fit} (top left), β_{spec} (top right), and R_β (bottom) for the sample. Filled rectangles are the radio-quiet sample, with the radio-loud sample overlotted as hatched rectangles.

different median. However, there is a probability of 93 percent that the distributions of both β_{spec} and R_β have different medians for radio-quiet and radio-loud groups, in the sense that β_{spec} is higher for RQ groups. This is not a strong result, because of the large errors on β_{spec} and therefore R_β . There is no evidence that RL groups have flatter profiles than RQ groups, as might be expected if the luminosity had been significantly decreased as a result of radio-galaxy input. In Section 4 we present further discussion of how the group density distribution might be affected by radio-galaxy energy input

3.4 Testing Model II: $L_X = L_B$ relation

The X-ray and optical luminosities of groups are correlated, because gas mass and galaxy mass should scale similarly. OP04 show

that such a correlation exists for their sample. If the effects we observe in Fig. 2 are caused by a decrease in X-ray luminosity in the radio-loud groups, then the $L_X = L_B$ relation should be affected: radio-loud groups should have a lower X-ray luminosity relative to their optical luminosity. In Fig. 5, we show the $L_X = L_B$ relation for radio-quiet and radio-loud groups (using $c1$ and r_{cut}). Unlike what is seen for the $L_X = T_X$ relation, there is no apparent difference in the two subsamples. We note that the radio luminosity will be related to L_B , which may introduce a slight bias, but this should not affect the X-ray-to-optical luminosity ratio of the radio-loud groups. Therefore, this is a strong argument against X-ray luminosity decrements in radio-loud groups, as the radio source should not affect the optical luminosity of the group.

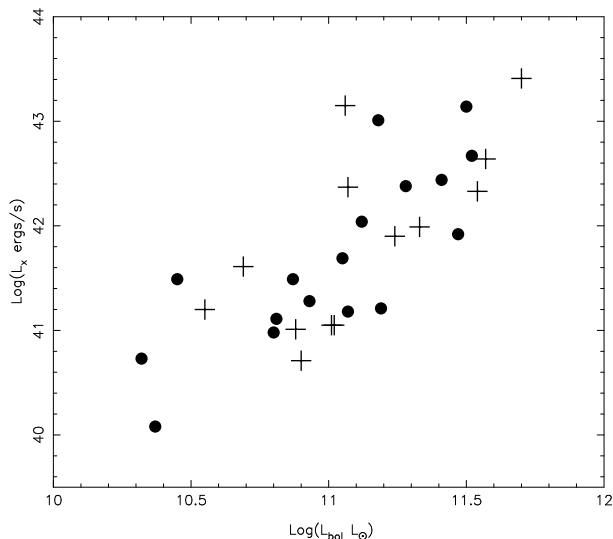


Figure 5. The $L_X = L_B$ relation for radio-quiet and radio-loud groups. Symbols are as for previous figures.

3.5 Testing Model III: optical properties of the RL and RQ subsamples

To test the possibility that radio-quiet and radio-loud groups are in different stages of evolution, so that an external mechanism might be causing the heating effect, we compared two measures of their optical properties. If radio-quiet groups are at a different stage of evolution from radio-loud groups, then N_{gals} , the number of galaxies in the group, might be expected to differ, in the sense that older groups might be expected to have fewer members. Older groups might also have a larger ratio between the brightest and second-brightest group galaxies, as the largest mergers should have already taken place. We therefore compared both N_{gals} and L_{12} , the luminosity ratio of the brightest to second-brightest group galaxy, as determined by OP04, for the two subsamples (using $c1$ and r_{cut}). In Fig. 6, we show histograms of the distribution of these parameters for the two subsamples. In neither case is there a significant difference in the distribution for the two subsamples. Both have a peak in the value of N_{gals} between 5 and 10, and the preferred value of L_{12} for both subsamples is < 2 , so that most groups have at least one reasonably large secondary galaxy, whether radio-loud or not. There are no radio-loud groups in the sample with $L_{12} > 10$, whereas there are two radio-quiet groups with $L_{12} > 20$. However, a K-S test indicates no significant difference in the distributions of either. A median test also finds no significant difference in the medians of the two subsamples for either parameter. We conclude that the galaxy distributions in radio-quiet and radio-loud elliptical-dominated groups are similar, so that there is no evidence that the two subsamples are at different evolutionary stages. However, a thorough investigation using more sophisticated measures of group history is required to test this model fully.

3.6 Chandra and XMM-Newton observations of heating and interactions in the RL groups

Many of the radio-loud groups in this sample have been observed with *Chandra* or *XMM-Newton*. The high resolution of *Chandra* is excellent for resolving an AGN component, and for detecting inner structure in groups; however, as a result of the high resolution, its

sensitivity to extended emission is reduced, so that in some cases it is unable to detect low surface-brightness emission from the weaker groups. In those cases *ROSAT* temperature and luminosity measurements are likely to be superior. We discuss here a few groups in the sample for which *Chandra* and *XMM-Newton* observations show evidence for heating or interactions between a radio-source and its environment.

3.6.1 NGC 4261

An *XMM-Newton* observation of this group was made on 16 December 2001 (ObsID 0056340101). An analysis of the extended emission has not yet been published, although Sambruna et al. (2003) presented an analysis of the nuclear emission. We extracted the archive *XMM-Newton* data and carried out standard processing and filtering as described in Croston et al. (2003). Fig. 7 shows the adaptively smoothed, background point-source subtracted, vignetting-corrected 0.5 – 5.0 keV image made from combined MOS1, MOS2 and pn data, with radio contours from a 1.4-GHz map made from VLA archive data overlaid. This figure illustrates a striking relationship between radio and X-ray morphology similar to that seen in 3C 66B (Croston et al. 2003). It is interesting that such evidence for interactions between the radio source and hot gas on large scales is found in every FRI radio galaxy for which deep *XMM* images of the large-scale structure exist [see also Evans et al. (2004)].

3.6.2 NGC 4636

The *Chandra* observation of the atmosphere surrounding NGC 4636 revealed striking substructure in the form of symmetrical bright arms (Jones et al. 2002). Jones et al. find that the leading edges of the arms are ~ 30 percent hotter than the surrounding gas, and postulate a model in which the arms are produced by shocks driven by symmetric off-centre AGN outbursts. The central radio source appears to be extended to the northeast and southwest (e.g. Birkinshaw and Davies 1985); however, it is small and too weak to have produced the shock-heating. Jones et al. argue that this indicates that a more direct nuclear outburst may have produced the shocks, but it is difficult to think of such a mechanism. The radio source could be more extended at low frequencies; however, it remains unlikely that a currently active radio source is producing the shocks. It is possible that a previous radio outburst is responsible, although it is unclear for how long the sharp density and temperature structure would persist. The shock-heated arms of gas in this group may be the main contributor to the overall temperature of 0.84 keV measured by *ROSAT*. As NGC 4636 has one of the largest temperature excesses, this example strongly suggests that we are indeed identifying groups with interesting AGN/group interactions.

3.6.3 NGC 1052

The *Chandra* observation is too short to detect much low surface-brightness emission from this poor group. However, as shown in Fig. 8, there is evidence for radio-related X-ray emission, as discussed by Kadler et al. (2004). They attribute most of the X-ray emission to the jet; however, the distribution of X-ray counts around the eastern radio lobe seems to be reminiscent of the bright shell of hot gas around the southwestern inner lobe of Centaurus A. The two systems are remarkably similar: they both consist of

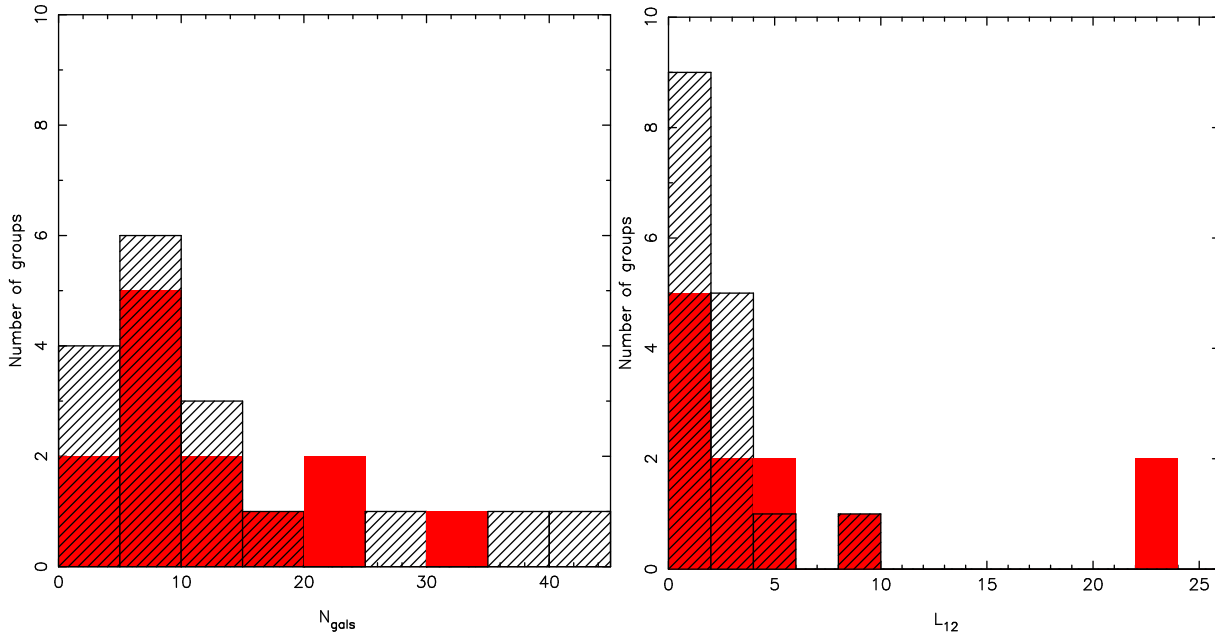


Figure 6. Histograms showing the distribution of N_{gals} (left) and L_{12} (right) for the radio-quiet and radio-loud samples. The RQ sample is indicated by filled rectangles, and the RL distribution is overplotted with hatched rectangles in both plots.

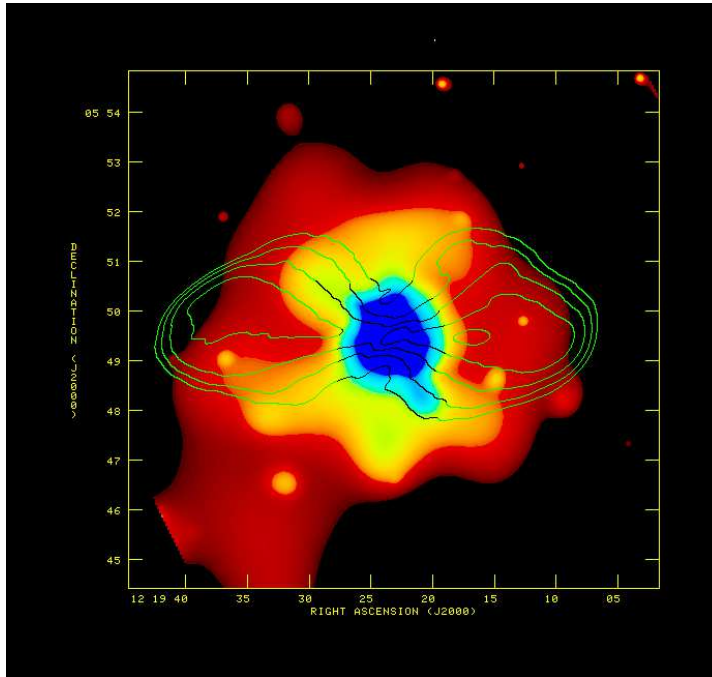


Figure 7. An adaptively smoothed, background point-source subtracted, vignetting-corrected 0.5 – 5.0 keV image of NGC 4261 made from the combined MOS1, MOS2 and pn data from the archive *XMM* observation described in the text. Clear evidence for interactions between the radio galaxy (3C 270) and gas environment are seen in the form of holes in the X-ray surface brightness at the positions of both radio lobes.

small, double-lobed radio sources, which are likely to be young or restarting. They have galaxy atmospheres of similar X-ray luminosities and temperatures. These *Chandra* observations therefore suggest that the young radio source in NGC 1052 may be shock-heating its surroundings. The measured X-ray temperature from *ROSAT* may contain a large contribution from these radio-related regions, although it is also possible that the entire environment has

been heated, as we have argued to be the case for 3C 66B (Croston et al. 2003).

3.6.4 HCG 62

The X-ray emission from HCG 62 provides one of the clearest examples of “holes” in a group atmosphere (Vrtilek et al. 2000). How-

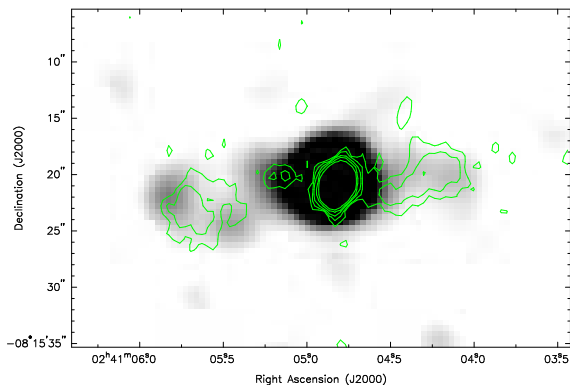


Figure 8. Gaussian smoothed image of the *Chandra* data for NGC 1052 in the energy range 0.5 – 5.0 keV. Radio contours are overlaid from a map made from archive VLA data (Wrobel 1984).

ever, the current AGN is a weak radio emitter, and does not show any extension. As with NGC 4636, it is plausible that a previous radio outburst (which may still be detectable in low-frequency radio observations) has produced the observed X-ray structure.

3.6.5 NGC 5044

This group shows prominent substructure in the *Chandra* image of Buote et al. (2003), who associate holes in the gas with the radio source. Although the NVSS image of this source does not show evidence for any extended radio emission, they suggest that observations at lower frequency might reveal the presence of radio emission filling the cavities. We have been unable to resolve the AGN or detect larger-scale radio emission in our analysis of VLA archive data.

3.6.6 Summary of the Chandra and XMM-Newton observations

The *Chandra* and *XMM-Newton* observations discussed above show that radio-source/group interactions are complex. In two cases, NGC 1052 and NGC 4261, there is clear evidence that the X-ray structure has been affected by the current radio galaxies. In two groups where there are no detected large-scale radio lobes, HCG 62 and NGC 4636, the *Chandra* observations reveal striking X-ray morphologies suggestive of outbursts from the AGN. Smaller-scale substructure is also present in NGC 5044. Finally, localised heating appears to be present in NGC 1052 and NGC 4636, suggesting that the heating effects we observe from the *ROSAT* sample could be caused by several different processes.

4 EVIDENCE FOR RADIO-SOURCE HEATING?

The results presented in Section 2 support the argument that radio galaxies have an important effect on the X-ray properties, and therefore the physical conditions, of group gas, as suggested by previous work (e.g. Croston et al. 2003). This is shown by the difference in $L_X = T_X$ properties of the two subsamples, and by the high incidence of radio-related substructure in radio-loud groups.

In the next two sections we discuss the three models of Section 3 in detail. In Section 4.1, we compare models I and II, and argue in favour of a radio-source heating model (Model I) and against a luminosity deficit (Model II). In Section 4.2, we consider one

possible external mechanism that could lead to a Model III explanation, that of mergers and interactions, and argue against such a model. In Section 4.3, we attempt to explain the results for all of the radio-loud groups in the context of a model of radio-source heating and discuss what can be inferred about the heating processes.

4.1 Temperature increase vs. luminosity decrement

Radio galaxies must displace large amounts of gas and this could have a significant effect on their luminosity. For 3C 66B, which is larger than most of the sources in the samples studied here, we calculated that the gas with which the radio source can have directly interacted provides only 7 percent of the group’s luminosity (Croston et al. 2003). It is therefore unlikely that removal of gas by the radio galaxy could produce the luminosity deficits needed by this model, in some cases an order of magnitude in luminosity. However, the group luminosity will also be decreased if a significant fraction of the jet kinetic energy is transferred into potential energy.

In the context of preheating models of energy injection into group gas, it has been argued (e.g. Metzler and Evrard 1994; Helsdon and Ponman 2000) that the main effect of the energy injection will be an increase in the group’s potential energy, so that the central density decreases (and hence luminosity will decrease). While (by the virial theorem) this will eventually be the case, heating effects are still likely to be detectable on shorter timescales. More recently, Kay (2004) has carried out cosmological simulations of cluster formation including cooling and feedback (which could be due to AGN or a different energy source such as supernova winds) and find gas properties in agreement with observations, with a 10 percent increase in temperature at the virial radius. Their simulations consider only massive clusters, but suggest that at least some fraction of AGN-injected energy is likely to end up in the thermal energy of the group.

In some of the groups in our sample an order of magnitude decrease in luminosity is required: the density would have to be dramatically reduced to produce such an effect. A strong argument against such large luminosity deficits in radio-loud groups comes from the $L_X = L_B$ relation discussed in Section 3.4. We find that the radio-loud groups follow the same trend as the radio-quiet groups and show no evidence for having lower X-ray luminosities relative to their optical luminosities, as would be expected if an X-ray luminosity decrease had been caused by the radio galaxy.

Another strong argument in favour of heating as the dominant effect, as opposed to a change in luminosity, is the result of Section 3.2, where we found evidence for a correlation between radio luminosity and the energy required to heat the gas from the predicted to the observed temperature. This result would be harder to explain in a model where the radio-source’s impact was principally on the group’s luminosity.

As shown in Section 3.6, several groups with a temperature excess possess additional evidence for radio-source heating. In Fig. 9, we show the $L_X = T_X$ relation for $c1$ and r_{cut} , with NGC 4636 and NGC 1052, as well as 3C 66B, 3C 449 and NGC 6251 (Croston et al. 2003; Evans et al. 2004) marked to illustrate how they compare to the sample studied here. We conclude, based on the additional evidence for heating in several sources, and the arguments above, that heating is a more plausible explanation than a radio-source induced luminosity deficit.

On the longest timescales, the energy injected by radio galaxies into group or cluster gas must predominantly end up as potential energy, and any long-term temperature increase will be small.

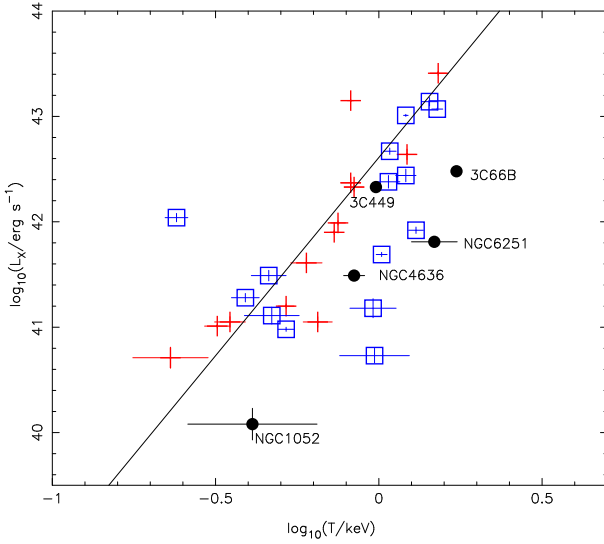


Figure 9. $L_X = T_X$ relation (c1, r_{cut}) showing the positions of the three *XMM*-observed radio-galaxy environments presented in Croston et al. (2003) and Evans et al. (2004), as well as the two OP04 groups with additional strong evidence for heating, NGC 1052 and NGC 4636, marked. + symbols indicate radio-quiet groups, and hollow squares radio-loud groups.

However, information about the energy injection cannot travel faster than the sound speed, so that temperature effects may be detectable for a few sound-crossing times. That an $L_X = T_X$ relation for elliptical-dominated groups exists at all is evidence that, on average, the temperature increase must disappear on timescales less than the radio-source recurrence time; for a 50 per cent radio-galaxy duty cycle, this is comparable to a few sound crossing times in a typical group. It is plausible that occasionally a second AGN outburst would occur before the group has recovered from the previous outburst, so that the temperature increase is more persistent; 3C 66B could be one example of such a system. Our results therefore suggest that we are detecting the short-term effects of radio-source heating in many elliptical-dominated groups. The fact that we have found no systematic differences in the properties of radio-loud and radio-quiet groups, other than their $L_X = T_X$ relations, is consistent with a model in which all elliptical-dominated groups have had similar numbers of radio-galaxy outbursts averaged over the group lifetime, affecting the groups by causing a temporary increase in temperature, with less easily detectable long-term effects on the group luminosity and surface brightness distribution.

4.2 The evolution of groups: a common cause for heating and radio activity?

An alternative explanation is that some common cause triggers a radio source and heats the gas. It is possible that the elliptical-dominated groups containing radio sources exist at a particular stage in the evolutionary process for groups, where the gas is hotter relative to the group luminosity. One possibility is that the incidence of mergers, and/or the type of mergers that the two subsamples of groups have undergone, is different for the two subsamples.

Recent simulations by Rowley et al. (2004) find that in *major* mergers (defined as increasing the cluster mass by 20 per cent) clusters become brighter and heat up roughly parallel to the $L_X = T_X$ relation, whereas in minor mergers, the temperature increases and the luminosity decreases. Although these simulations

are for more massive clusters, this suggests a possible interpretation of our results. If the radio-loud groups had recently undergone, or are continuing to undergo, minor mergers, then their $L_X = T_X$ properties could be explained. In this model, the radio-quiet groups must either have undergone mainly major mergers, or be in more isolated environments where mergers are less common. One possibility is that radio-quiet groups could be more evolved, so that most merging has already occurred, and the gas has cooled back to the $L_X = T_X$ line. In this scenario, it might be expected that the radio-quiet groups would resemble fossil groups where mergers are no longer common.

Such a model of group evolution should be testable using the optical properties of the group. However, we found no evidence for a difference in either the number of galaxies in the group or the degree of dominance by the central galaxy for the radio-quiet and radio-loud groups (Section 3.5). A model of this sort cannot be ruled out, as mergers remain the most plausible model for how radio galaxies are triggered. However, there does not appear to be any evidence that the radio-quiet and radio-loud groups are in different stages of evolution, based on the comparison of the optical group properties. We therefore conclude that radio-source heating is the most plausible of the three explanations for our results.

4.3 Models for radio-source heating

If the radio-source heating model is adopted, then it is necessary to consider whether it is possible to explain the observed results for all of the radio-loud groups in the context of this model. In Fig. 2, it is apparent that there are some “radio-loud” groups that do not show a temperature excess, and one particularly anomalous group that is much cooler than predicted (NGC 3557). In addition to the sources with no large temperature excess, most of the currently active radio sources in the sample are unlikely to be capable of producing all of the heating that is observed. The two groups HCG 62 and NGC 4636, which show strong evidence for radio-related structure and a large heating effect (especially in the latter), are particularly problematic. Either there is low-frequency radio structure that has not yet been observed, which indicates active or recently switched-off large-scale radio jets and lobes, or else the heating effects are long-lived. Some of the most powerful radio sources, such as 3C 66B, 3C 449, and NGC 4261, are probably capable of producing the heating that is observed (Croston et al. 2003), but the heating in many of the radio-loud groups must be longer-lived than the radio source.

It is also interesting to consider the mechanisms for heating in different stages of radio-source evolution. In Croston et al. (2003), we argued that large, powerful FRIs are subsonic and likely to be heating their surroundings gently via $P dV$ work as the lobes expand. However, in the early stages of FRI evolution, the sources are known to be overpressured (even assuming minimum energy pressures), and the recent observation of a heated shell around the inner lobe of Cen A shows that shock-heating is not only likely to be an important mechanism in FRIIs, but plays a role in the early stages of FRI evolution as well. This process may also be occurring in one of the groups in this sample, NGC 1052 (see Section 3.6.3). Finally, the *Chandra* observations of NGC 4636 show that additional mechanisms for AGN heating may exist, as it is difficult to explain the morphology of the shocked arms of gas via radio-lobe expansion. We conclude that the heating effects found in the study of the *ROSAT* sample presented here are likely to be the result of different types of radio-source heating, so that one simple model for the entire sample is unlikely to be correct. In some sources there

may be small regions of shocked gas, unresolved in the *ROSAT* data, leading to the temperature increases, whereas in others more widespread heating is necessary. A detailed analysis of *XMM* observations, which now exist for a significant number of the radio-loud groups, would help to investigate these possibilities, as would a low-frequency radio study to constrain the properties of the radio sources.

4.4 The importance of radio galaxies in structure formation models

We have shown that radio galaxies at some stage of development are present in up to 50 percent of elliptical-dominated groups (Section 2.3), and have also presented evidence that radio-source heating is common. It is therefore of interest to consider whether their energy input is of significance in the context of structure formation models. We carried out some simple calculations to determine whether the energy input from low-power radio sources in elliptical-dominated groups could be important in the context of the energy-injection requirements of structure formation models.

We estimated the energy input rate from the average radio source in the sample by taking the average value of $L_{1.4}$ for the 19 radio-loud groups ($3.5 \times 10^{23} \text{ W Hz}^{-1}$) and scaling the kinetic luminosity of 3C 31 (from the model of Laing and Bridle 2002) by the ratio of $L_{1.4}$ for the average radio source and 3C 31, which gives $7 \times 10^{35} \text{ W}$. We then assumed that 1/3 of the kinetic luminosity is transferred to the group gas, a conservative lower limit. We assumed a duty cycle of 50 percent, based on the fraction of radio sources in the Garcia catalogue (Section 2.3). This gives a typical energy input rate of $2.3 \times 10^{51} \text{ keV/s}$ over the lifetime of the group. The energy rate per particle was determined using the average number of particles in the group (determined as part of the heat capacity calculations in Section 3.2) to be $6.6 \times 10^{18} \text{ keV/particle/s}$. Assuming the injection energy is required to be of order 1 keV/particle (e.g. Wu et al. 2000), then the average radio source in the sample can provide the necessary energy input over 5×10^9 years, which is a plausible group lifetime (this is about 10 times the standard radio-galaxy lifetime, so that the radio source must have ~ 5 active phases during the group lifetime). We conclude that low-power radio sources may be capable of providing the necessary energy input in elliptical-dominated groups. As it is the elliptical-dominated groups that principally determine the $L_X = T_X$ relation for groups, since they dominate the population of groups with luminous, group-scale X-ray environments, it is therefore possible that the energy input from *low-power* radio galaxies can explain the X-ray properties of groups.

Other workers have carried out calculations of the energy input of radio galaxies into clusters. It seems likely that low-power radio galaxies can provide sufficient energy on average to balance cooling flows (e.g. Fabian et al. 2003); however, to explain the cluster $L_X = T_X$ relation may require more energy than can be supplied by FRIs [although Roychowdhury et al. (2004) found that effervescent heating by rising bubbles could solve the entropy problem by heating at large radii]. The energy contribution from FR II radio galaxies and quasars is also likely to be important in the rarer situations where they occur.

5 CONCLUSIONS

We have presented a detailed study of the gas properties of radio-quiet and radio-loud elliptical-dominated groups based on the

ROSAT groups sample of Osmond & Ponman (2004). We reach the following conclusions:

63 percent of the elliptical-dominated groups (19/30) in the OP04 sample have associated radio sources at the centre of a dominant group galaxy.

Our sample of elliptical-dominated groups is not significantly biased in its radio-loud fraction: the true fraction in the parent population may be ~ 40 –50 per cent.

Radio-loud groups are likely to have a higher temperature than radio-quiet groups of the same luminosity.

The energy required to produce the observed temperature excess correlates weakly with the 1.4-GHz radio luminosity of the sources.

The difference in gas properties for radio-quiet and radio-loud groups is most plausibly interpreted as evidence for radio-source heating.

Evidence for radio-source interactions with the surrounding gas is found in *Chandra* or *XMM-Newton* observations of many of the radio-loud groups, although there are also several groups that show disturbances not directly related to observable radio structure.

The radio-loud groups are at different stages in the heating process, so that some may be experiencing shock-heating by young radio sources, some are being gently heated by a currently active large radio galaxy, and some show longer-lived heating effects from a previous generation of radio-source activity.

ACKNOWLEDGMENTS

We are grateful to Trevor Ponman for providing access to the GEMS X-ray analysis in advance of publication, and for helpful comments in the course of JHC's PhD viva. We would also like to thank Diana Worrall for comments on an early draft, and to thank the referee for helpful suggestions. JHC thanks PPARC for a studentship. MJH thanks the Royal Society for a research fellowship. This work made use of the NASA/IPAC Extragalactic Database (NED), which is operated by the Jet Propulsion Laboratory, California Institute of Technology, under contract with the National Aeronautics and Space Administration.

REFERENCES

- Arnaud, M. and Evrard, A. E.: 1999, *MNRAS* **305**, 631
- Böhringer, H., Matsushita, K., Churazov, E., Ikebe, Y., and Chen, Y.: 2002, *A&A* **382**, 804
- Balogh, M. L., Babul, A., and Patton, D. R.: 1999, *MNRAS* **307**, 463
- Becker, R. H., White, R. L., and Helfand, D. J.: 1995, *ApJ* **450**, 559
- Benson, A. J., Bower, R. G., Frenk, C. S., Lacey, C. G., Baugh, C. M., and Cole, S.: 2003, *ApJ* **599**, 38
- Best, P. N.: 2004, *MNRAS* **351**, 70
- Binney, J. and Tabor, G.: 1995, *MNRAS* **276**, 663
- Birkinshaw, M. and Davies, R. L.: 1985, *ApJ* **291**, 32
- Blanton, E. L., Sarazin, C. L., McNamara, B. R., and Wise, M. W.: 2001, *ApJ* **558**, L15
- Böhringer, H., Voges, W., Fabian, A. C., Edge, A. C., and Neumann, D. M.: 1993, *MNRAS* **264**, L25
- Brüggen, M. and Kaiser, C. R.: 2001, *MNRAS* **325**, 676
- Brüggen, M. and Kaiser, C. R.: 2002, *Nature* **418**, 301
- Brighenti, F. and Mathews, W. G.: 2001, *ApJ* **553**, 103

- Buote, D. A., Lewis, A. D., Brighenti, F., and Mathews, W. G.: 2003, *ApJ* **594**, 741
- Churazov, E., Brüggén, M., Kaiser, C. R., Böhringer, H., and Forman, W.: 2001, *ApJ* **554**, 261
- Cole, S.: 1991, *ApJ* **367**, 45
- Condon, J. J., Cotton, W. D., Greisen, E. W., Yin, Q. F., Perley, R. A., Taylor, G. B., and Broderick, J. J.: 1998, *AJ* **115**, 1693
- Croston, J. H., Hardcastle, M. J., Birkinshaw, M., and Worrall, D. M.: 2003, *MNRAS* **346**, 1041
- de Vaucouleurs, G., de Vaucouleurs, A., Corwin, H. G., Buta, R. J., Paturel, G., and Fouque, P.: 1991, *Third Reference Catalogue of Bright Galaxies*, Volume 1-3, XII, 2069, Springer-Verlag New York
- Eilek, J. A.: 2004, in *The Riddle of Cooling Flows in Galaxies and Clusters of galaxies*, Eds. T. Reiprich, J. Kempner, and N. Soker. To be published electronically at <http://www.astro.virginia.edu/coolflow/>
- Evans, D. A., Hardcastle, M. J., Croston, J. H., Worrall, D. M., and Birkinshaw, M.: 2004, *MNRAS*, *submitted*.
- Fabian, A. C., Sanders, J. S., Allen, S. W., Crawford, C. S., Iwasawa, K., Johnstone, R. M., Schmidt, R. W., and Taylor, G. B.: 2003, *MNRAS* **344**, L43
- Garcia, A. M.: 1993, *A&AS* **100**, 47
- Hardcastle, M. J., Worrall, D. M., Birkinshaw, M., Laing, R. A., and Bridle, A. H.: 2002, *MNRAS* **334**, 182
- Helsdon, S. F. and Ponman, T. J.: 2000, *MNRAS* **315**, 356
- Ho, L. C.: 1999, *ApJ* **510**, 631
- Isobe, T., Feigelson, E. D., Akritas, M. G., and Babu, G. J.: 1990, *ApJ* **364**, 104
- Jones, C., Forman, W., Vikhlinin, A., Markevitch, M., David, L., Warmflash, A., Murray, S., and Nulsen, P. E. J.: 2002, *ApJ* **567**, L115
- Kadler, M., Kerp, J., Ros, E., Falcke, H., Pogge, R. W., and Zensus, J. A.: 2004, *A&A* **420**, 467
- Kay, S. T.: 2004, *MNRAS* **347**, L13
- Kraft, R. P., Kregenow, J. M., Forman, W. R., Jones, C., and Murray, S. S.: 2001, *ApJ* **560**, 675
- Kraft, R. P., Vázquez, S. E., Forman, W. R., Jones, C., Murray, S. S., Hardcastle, M. J., Worrall, D. M., and Churazov, E.: 2003, *ApJ* **592**, 129
- Kravtsov, A. V. and Yepes, G.: 2000, *MNRAS* **318**, 227
- Laing, R. A. and Bridle, A. H.: 2002, *MNRAS* **336**, 1161
- Lavalley, M., Isobe, T., and Feigelson, E.: 1992, in *ASP Conf. Ser. 25: Astronomical Data Analysis Software and Systems I*, pp 245–
- Metzler, C. A. and Evrard, A. E.: 1994, *ApJ* **437**, 564
- Osmond, J. P. F. and Ponman, T. J.: 2004, *MNRAS* **350**, 1511
- Peterson, J. R., Kahn, S. M., Paerels, F. B. S., Kaastra, J. S., Tamura, T., Bleeker, J. A. M., Ferrigno, C., and Jernigan, J. G.: 2003, *ApJ* **590**, 207
- Ponman, T. J., Cannon, D. B., and Navarro, J. F.: 1999, *Nature* **397**, 135
- Reynolds, C. S., Heinz, S., and Begelman, M. C.: 2002, *MNRAS* **332**, 271
- Rowley, D. R., Thomas, P. A., and Kay, S. T.: 2004, *MNRAS*, *in press*.
- Roychowdhury, S., Ruszkowski, M., Nath, B. B., and Begelman, M. C.: 2004, *ApJ*, *in press*; *astro-ph/0401161*
- Sadler, E. M., Jackson, C. A., Cannon, R. D., McIntyre, V. J., Murphy, T., Bland-Hawthorn, J., Bridges, T., Cole, S., Colless, M., Collins, C., Couch, W., Dalton, G., De Propriis, R., Driver, S. P., Efstathiou, G., Ellis, R. S., Frenk, C. S., Glazebrook, K., Lahav, O., Lewis, I., Lumsden, S., Maddox, S., Madgwick, D., Norberg, P., Peacock, J. A., Peterson, B. A., Sutherland, W., and Taylor, K.: 2002, *MNRAS* **329**, 227
- Sakelliou, I., Peterson, J. R., Tamura, T., Paerels, F. B. S., Kaastra, J. S., Belsole, E., Böhringer, H., Branduardi-Raymont, G., Ferrigno, C., den Herder, J. W., Kennea, J., Mushotzky, R. F., Vestrand, W. T., and Worrall, D. M.: 2002, *A&A* **391**, 903
- Sambruna, R. M., Gliozzi, M., Eracleous, M., Brandt, W. N., and Mushotzky, R.: 2003, *ApJ* **586**, L37
- Schmidt, M.: 1978, *Phys. Scr* **17**, 135
- Smith, D. A., Wilson, A. S., Arnaud, K. A., Terashima, Y., and Young, A. J.: 2002, *ApJ* **565**, 195
- Voigt, L. M. and Fabian, A. C.: 2004, *MNRAS* **347**, 1130
- Voigt, L. M., Schmidt, R. W., Fabian, A. C., Allen, S. W., and Johnstone, R. M.: 2002, *MNRAS* **335**, L7
- Voit, G. M. and Bryan, G. L.: 2001, *Nature* **414**, 425
- Vrtilek, J. M., David, L. P., Grego, L., Jerius, D., Jones, C., Forman, W., Donnelly, R. H., and Ponman, T. J.: 2000, in *Constructing the Universe with Clusters of Galaxies*, available at <http://www.iap.fr/Conferences/Colloque/coll2000/contributions>.
- Worrall, D. M., Birkinshaw, M., and Hardcastle, M. J.: 2003, *MNRAS* **343**, L73
- Wrobel, J. M.: 1984, *ApJ* **284**, 531
- Wu, K. K. S., Fabian, A. C., and Nulsen, P. E. J.: 2000, *MNRAS* **318**, 889
- Zhang, Z. and Xu, H.: 2004, *Chinese Journal of Astronomy and Astrophysics* **4**, 221